BIOCHEMISTRY
including biophysical chemistry & molecular biology
Article

Biochemistry **2009,** *48,* 6111–6115 6111
DOI: 10.1021/bi900414k

Flash-Induced Structural Dynamics in Photosystem II Membrane Fragments of Green Plants[†]

Jörg Pieper* and Gernot Renger

Max-Volmer-Laboratories for Biophysical Chemistry, Technische Universitat Berlin, Strasse des 17. Juni 135, 10623 Berlin, Germany

Received March 13, 2009; Revised Manuscript Received May 6, 2009

ABSTRACT: Time-resolved quasielastic neutron scattering with laser excitation is a promising novel pump−probe approach, which opens up new perspectives for the study of protein−membrane dynamics in specific functional states of even complex systems. This is demonstrated here for the case of photosystem II membrane fragments with inhibited electron transfer. In contrast to the case of the model system bacteriorhodopsin, a transient reduction of the dynamics is observed ∼160 μs after the actinic laser flash. This effect is the first observation of a modulated structural dynamics in photosystem II membrane fragments.

The functional competence of proteins is often correlated with their internal flexibility based on diffusive protein motions on the picosecond time scale (*1*−*4*). One prominent example is electron transfer in the multimeric protein complex photosystem II (PS II)[1] (see Figure 1), which functions as a light-driven water-plastoquinone oxidoreductase (*5*). Light absorption occurring primarily in antenna pigment-protein complexes (labeled b and c in Figure 1) leads to a primary charge separation in the PS II reaction center (labeled a in Figure 1). The primary charge separation is subsequently stabilized via a sequence of electron transfer steps to a permanently bound plastoquinone molecule Q_A, thus forming the "stable" radical pair $P680^{+\bullet}Q_A^{-\bullet}$ (see ref (*6*) and references therein). $P680^{+\bullet}$ provides the driving force for oxidative photosynthetic water splitting at the donor side of PS II (see, e.g., ref (*7*)), while $Q_A^{-\bullet}$ is the reductant for plastoquinol formation at the acceptor side of PS II. The latter process involves further electron transfer to a transiently bound plastoquinone molecule Q_B and coupled proton uptake reactions (for a review, see ref (*8*)). The $Q_A^{-\bullet} \rightarrow Q_B$ electron transfer is generally a multiexponential process but exhibits a major ∼160 μs time constant. Interestingly, the reoxidation of $Q_A^{-\bullet}$ by Q_B is completely blocked below ∼200 K (*9*, *10*). This observation of a thermal "freezing" of the $Q_A^{-\bullet}$ reoxidation indicates a crucial role of structural flexibility for the PS II functionality.

Protein dynamics in PS II membrane fragments from spinach has already been investigated by quasielastic neutron scattering (QENS), which makes use of the large incoherent scattering cross section of protons and of their quasiuniform distribution in biomolecules so that hydrogen motions are utilized as a probe of protein dynamics. The onset of diffusive protein motions with characteristic relaxation times in the picosecond range was observed with a "dynamical transition" at ∼240 K (*11*), and at a relative humidity (rh) of ∼45% at room temperature (*12*). The latter effects were shown to be strictly correlated with the temperature- and hydration-dependent increase in the electron transport efficiency from $Q_A^{-\bullet}$ to Q_B (*10*). So far, however, these correlations between dynamics and function in PS II have been established by comparison of independent experiments.

The first direct observation of a functionally modulated dynamics via employment of a novel type of (light-neutron) pump−probe experiment, which combined in situ optical activation of the photocycle of the model system bacteriorhodopsin (BR) with a time-selective test of its dynamics using QENS, has just recently been reported (*4*). A transient softening of the protein during the photocycle of BR was observed on the millisecond time scale, which most probably promotes the large-scale structural change in the M intermediate of BR. This approach appears to be highly promising also for the investigation of complex systems like PS II, because the relevant dynamics of specific functional states can be isolated. In addition to electron and slower proton transfer in the PS II reaction center, structural dynamics may also be influenced by the dynamics of excited electronic states (*13*) and reversible structural changes in the PS II antenna proteins associated with photoprotective mechanisms (*14*, *15*).

In this study, we present the first application of laser-excited QENS to hydrated stacks of PS II membrane fragments as schematically shown in the inset of Figure 1. To reduce

[†]Financial support by Deutsche Forschungsgemeinschaft (SFB 429, TP A1) is gratefully acknowledged.

*To whom correspondence should be addressed: Technische Universitat Berlin, PC14, Strasse des 17. Juni 135, 10623 Berlin, Germany. Telephone: +49-30-31421067. Fax: +49-30-31421122. E-mail: joerg.pieper@tu-berlin.de.

[1]Abbreviations: QENS, quasielastic neutron scattering; PS II, Photosystem II; rh, relative humidity; Chl, chlorophyll; HWHM, half-width at half-maximum; fwhm, full width at half-maximum; EISF, elastic incoherent structure factor; QISF, quasielastic incoherent structure factor; DHO, damped harmonic oscillator; LHC II, light-harvesting complex II.

Published on Web 05/08/2009

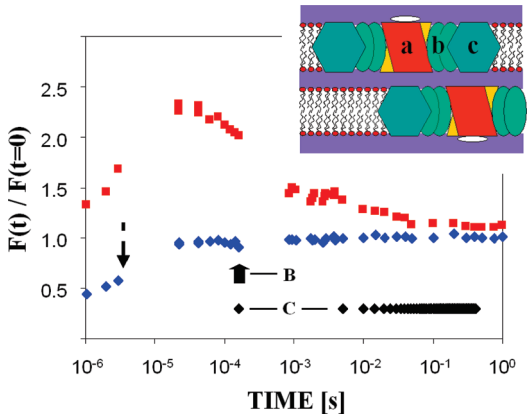

FIGURE 1: Flash-induced fluorescence quantum yield of an intact spinach leaf (red squares) and PSII membrane fragments with inhibited $Q_A^{-\bullet} \rightarrow Q_B$ electron transfer hydrated at 90% rh (blue diamonds). The second data set was obtained directly at a PSII sample used for light-excited QENS experiments. A broken arrow indicates the rise of the fluorescence quantum yield due to $P680^{+\bullet}$ reduction and the decay of ^{3}Car. The actinic laser flashes at $t = 0$ had a wavelength of 532 nm and a pulse energy of 8 mJ/cm^2. A thick black arrow shows a probe pulse delay of ~160 μs (experimental regime B), while black diamonds indicate the temporal position of all neutron pulses (regime C). The inset (right upper corner) shows a schematic view of the hydrated PSII membrane fragment system with a) reaction center, b) minor antennae, and c) major antenna complexes. The hydration water layers are indicated in blue.

complexity, experiments were performed on the timescale of ~160 μs using samples with inhibited $Q_A^{-\bullet} \rightarrow Q_B$ electron transfer.

MATERIALS AND METHODS

PS II membrane fragments were prepared from spinach (*Spinacea oleracea*) as described previously (*11*) and equilibrated using D_2O vapor of 90% relative humidity (rh). The absorbance of the sample was adjusted to ~1 at the excitation laser wavelength of 532 nm to ensure a sizable sample excitation. The typically small pool of Q_B acceptor molecules in PS II membrane fragments was fully reduced by laser excitation prior to fluorescence and QENS experiments, so that $Q_A^{-\bullet}$ reoxidation was inhibited. The samples were contained in vacuum-tight sample cells with sapphire windows, which are transparent to both visible excitation light and neutron probe pulses.

QENS characterizes protein−membrane dynamics via the measurement of energy and momentum exchange between the sample and low-energy (1 meV < E < 20 meV) neutrons (for a review, see ref (*2*)). This method is especially sensitive for picosecond reorientational motions of hydrogen atoms in small protein subgroups because of the exceptionally large incoherent neutron scattering cross section of protons and their almost homogeneous distribution in proteins.

In an incoherent QENS experiment, the measured quantity is the double-differential cross section (see, e.g., ref (*2*)), which describes the number of neutrons scattered into a space angle element $\delta\Omega$ and an energy transfer element $\delta\omega$

$$\frac{\delta^2\sigma}{\delta\Omega\delta\omega} = \frac{|\mathbf{k}_1|}{|\mathbf{k}_0|}[b_{inc}{}^2 S_{inc}(\mathbf{Q},\omega)] \quad (1)$$

where $\mathbf{k}_0$ and $\mathbf{k}_1$ are the wave vectors of incident and scattered neutrons, respectively, b_{inc} is the incoherent scattering length, $S_{inc}(\mathbf{Q},\omega)$ is the incoherent scattering function with $\mathbf{Q}$ being the momentum transfer defined by $\mathbf{Q} = \mathbf{k}_1 - \mathbf{k}_0$, and $\hbar\omega$ reflects the energy transfer. The function $S_{inc}(\mathbf{Q},\omega)$ is related to the Van Hove self-correlation function $G(\mathbf{r},t)$ by

$$S_{inc}(\mathbf{Q},\omega) = \frac{1}{2\pi}\int_{-\infty}^{\infty} e^{-i\omega t}\int_{-\infty}^{\infty} e^{i\mathbf{Q}r} G(\mathbf{r},t)\, d\mathbf{r}\, dt \quad (2)$$

where, in the classical approximation, $G(\mathbf{r},t)$ is the average time-dependent probability density distribution of the hydrogen atoms in the studied sample. In practice, $S_{inc}(\mathbf{Q},\omega)$ needs to be replaced by an experimental scattering function $S_{exp}(\mathbf{Q},\omega)$ with

$$S_{exp}(\mathbf{Q},\omega) = F_N \exp\left(-\frac{\hbar\omega}{2kT}\right) R(\mathbf{Q},\omega) \otimes S_{theo}(\mathbf{Q},\omega) \quad (3)$$

which is composed of a normalization factor F_N, the detailed balance factor $\exp[-\hbar\omega/2kT]$, and the convolution of an experimentally obtained resolution function $R(\mathbf{Q},\omega)$ with a theoretical scattering function $S_{theo}(\mathbf{Q},\omega)$ describing the dynamics of the sample system. Within this study, we employ a purely phenomenological approach for $S_{theo}(\mathbf{Q},\omega)$:

$$S_{theo}(\mathbf{Q},\omega) = e^{-\langle u^2\rangle Q^2}[A_0(\mathbf{Q})\delta(\omega) + \sum_n A_n(\mathbf{Q}) L_n(H_n,\omega) + S_{in}(\mathbf{Q},\omega)] \quad (4)$$

This theoretical scattering function consists of a $\delta(\omega)$-shaped elastic component, a sum of quasielastic Lorentzian terms, $L_n(H_n,\omega)$, with half-widths at half-maximum (HWHM) H_n, and an inelastic lineshape, $S_{in}(\mathbf{Q},\omega)$, described in detail in ref (*11*). The sum of fractional intensities $A_0(\mathbf{Q})$ and $A_n(\mathbf{Q})$ is normalized to unity, and they are termed the elastic (EISF) and quasielastic incoherent structure factors (QISF), respectively; $\exp(-\langle u^2\rangle Q^2)$ is the Debye−Waller factor with a vibrational mean square displacement $\langle u^2\rangle$.

Neutron experiments were conducted using the NEAT spectrometer at the Hahn-Meitner Institute Berlin (Berlin, Germany). The measurments were performed at room temperature (295 K) using a neutron wavelength of 5.1 Å (~3.2 meV) and an elastic Q range of 0.3−2.3 Å^{-1}. The elastic energy resolution (ΔE) was 93 μeV, corresponding to an observation time window from ~0.2 to ~20 ps. The setup for laser-excited QENS was described in detail in ref (*16*). Light-induced spectra were recorded using laser flashes with a wavelength of 532 nm and a pulse energy of 8 mJ/cm^2. The data were corrected for empty cell contribution, detector efficiency, normalized to the vanadium intensity, and converted to energy transfer scale using FITMO-4. The sample transmission was typically 99% so that multiple scattering effects should be negligible in the QENS data.

RESULTS AND DISCUSSION

Prior to laser-excited QENS experiments, the light-induced functional state of the PS II membrane fragment sample has been determined by time-resolved measurements of the normalized flash-induced fluorescence quantum yield using the setup described by Steffen et al. (*17*). In an intact leaf, a saturating laser flash at 532 nm with a pulse energy of 8 mJ/cm^2 induces the charge-separated state $P680^{+\bullet}Q_A^{-\bullet}$ in the PS II reaction center. Within the lifetime of $Q_A^{-\bullet}$, electronic excitations cannot trigger another "stable" charge separation and are dissipated via non-radiative and radiative emission, resulting in an increase in the overall fluorescence yield. In addition, the rise kinetics on the nano- to microsecond time scales is determined by both the $P680^{+\bullet}$ reduction and the decay of quenching carotenoid triplets

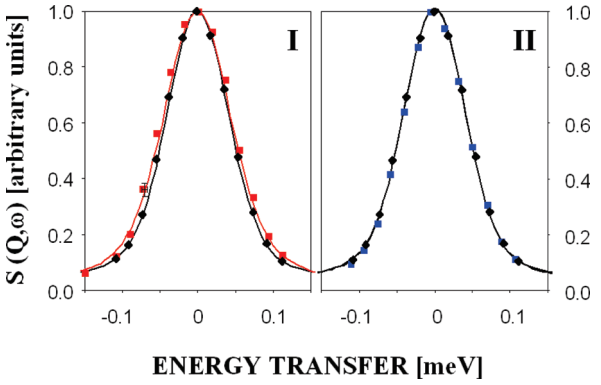

FIGURE 2: Quasielastic region of the flash-induced normalized QENS spectra of PS II membrane fragments (90% rh D_2O) obtained in the three experimental regimes: (A) in the dark (black), (B) selectively with a time delay of ~160 μs after the actinic laser flash (red), and (C) upon laser excitation, but averaged over all probe pulses (blue). Frame I shows a comparison of regimes A and B, exhibiting a light-induced difference ~160 μs after the laser flash. Frame II reveals that spectra obtained in regimes A and C are essentially similar. The black and red lines are fits according to eq 1. Error bars are given for one representative data point of the light-induced QENS spectrum, while the uncertainty is in the range of the symbol size for the black and blue QENS spectra, respectively.

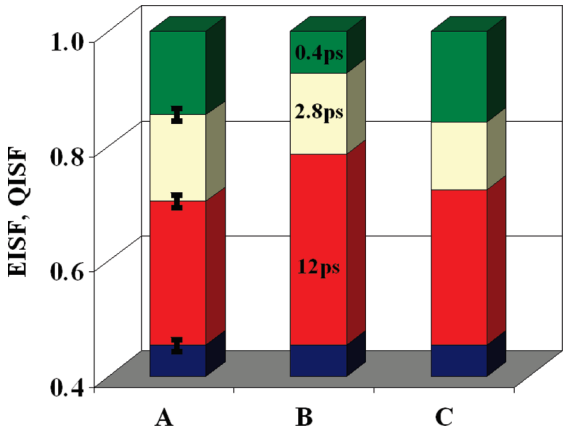

FIGURE 3: Elastic and quasielastic incoherent structure factors of PSII membrane fragments obtained from fits of the QENS spectra shown in Figure 2. The letters A−C refer to the respective fit functions of the three experimental regimes: (A) dark measurement, (B) light-excited measurement selectively ~160 μs after the laser flash, and (C) light-excited measurement averaged over all neutron probe pulses. The elastic incoherent structure factor is colored blue, and the quasielastic incoherent structure factors are colored red (τ_1 = 12 ps), yellow (τ_2 = 2.8 ps), and green (τ_3 = 0.4 ps). The black bars in the left column indicate the uncertainty of the fit parameters.

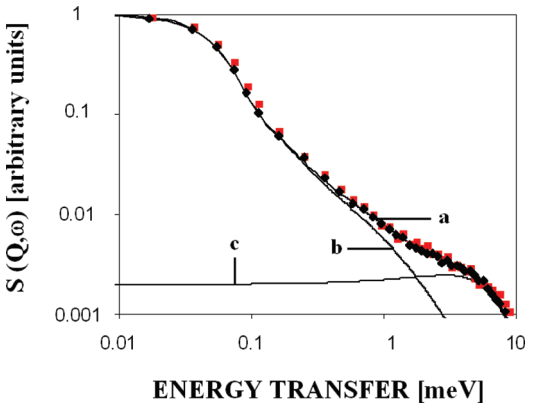

FIGURE 4: Double-logarithmic plot of the flash-induced normalized QENS spectra of Figure 2 obtained in regimes A and B, i.e., in the dark (black) and ~160 μs after the laser flash (red), revealing that the QENS spectra are widely similar in the inelastic scattering region. The black lines are (a) the fit function $S(\mathbf{Q},\omega)$ according to eq 1 and (b) the quasielastic and (c) the inelastic contribution to the fit.

(^{3}Car). The subsequent decay of the fluorescence yield mainly reflects the $Q_A^{-\bullet} \rightarrow Q_B$ electron transfer. The transients of the flash-induced fluorescence changes are monitored by a series of weak probe light pulses and fitted by a model that takes into account three effects occurring on the time scale of the experiment: (a) quenching of fluorescence due to formation of $P680^{+\bullet}$ and carotenoid triplets (^{3}Car), (b) recombination of $P680^{+\bullet}Q_A^{-\bullet}$, and (c) $Q_A^{-\bullet} \rightarrow Q_B$ electron transfer (*17*). The flash-induced normalized fluorescence quantum yield changes of an intact spinach leaf shown in Figure 1 (see red squares) exhibit the expected increase of the quantum yield due to population of state P680 $Q_A^{-\bullet}$ followed by a decay with a major 160 μs time constant due to $Q_A^{-\bullet}$ reoxidation. An experiment on PS II membrane fragments conducted under the same experimental conditions (see the blue diamonds in Figure 1) does not reveal the characteristics of $Q_A^{-\bullet}$ formation and $Q_A^{-\bullet} \rightarrow Q_B$ electron transfer. Rather, the data can be fully explained by formation and decay of carotenoid triplet states (^{3}Car), leading to an enhanced nonradiative decay of excitation energy (see the broken arrow in Figure 1). Thus, the laser-induced QENS spectra presented below are not correlated with conformational changes due to $Q_A^{-\bullet}$ reoxidation but rather reflect dynamical modulations of protein mobility occurring on the same time scale.

Light-excited QENS spectra of PS II membrane fragments were obtained in three experimental regimes, as described in ref (*4*): (A) dark measurement, (B) experiment under illumination probing selectively ~160 μs after laser excitation, and (C) experiment under illumination, but averaging over all neutron probe pulses. The data sets are generally described by the model scattering function $S_{theo}(\mathbf{Q},\omega)$ according to eq 4. In the following, the fit functions obtained are labeled according to the three experimental regimes A, B, and C as $S_A(\mathbf{Q},\omega)$, $S_B(\mathbf{Q},\omega)$, and $S_C(\mathbf{Q},\omega)$.

A satisfactory fit of the QENS spectrum in the dark (see the black diamonds in Figure 2) requires at least three quasielastic components representing localized diffusive protein motions with mean relaxation times τ_1 (12 ps), τ_2 (2.8 ps), and τ_2 (0.4 ps), respectively. The inelastic line shape $S_{in}(\mathbf{Q},\omega)$ is given by a damped harmonic oscillator (DHO) function with an energy of 6.5 meV and a damping of 10 meV similar to that used for PS II membrane fragments in ref (*11*). In the following, the light-induced QENS spectra will be described by variation of only the EISF and QISFs of the quasielastic components (see Figure 3 for parameters).

The light-induced QENS spectrum of PS II membrane fragments shown in frame I of Figure 2 (red squares) was obtained selectively ~160 μs after laser excitation. The temporal position of the neutron probe pulses is indicated by an arrow in Figure 1. The light-induced QENS spectrum reveals a statistically significant deviation from the dark spectrum mainly in the region of small energy transfers (ΔE < 0.1 meV) close to the elastic peak. If the two data sets are normalized to their peak intensities as in frame I of Figure 2, the difference appears as a broadening of the elastic peak. Generally, this finding indicates an increase in the fractional intensity of relatively slow motions. A fit employing the model scattering function $S_B(\mathbf{Q},\omega)$ shows that an increase in

the fractional intensity of the slow 12 ps component occurs mainly on the expense of the fast 0.4 ps term (see the QISF values in Figure 3), which is equivalent to a slowing of internal motions of PS II membrane fragments. In this regard, it is important that instead of an arbitrary flat background, the model scattering function involves a realistic line shape for an inelastic vibrational contribution, which leads to a proper normalization of the sum of the elastic and quasielastic intensities.

In contrast to the effect observed at small ΔE values, the QENS spectra are essentially similar in the inelastic scattering region with a ΔE of > 0.1 meV (see the double-logarithmic plot in Figure 4). As a consequence, the $\langle u^2 \rangle$ value of 0.065 $Å^{-2}$ remains constant for all QENS spectra of PS II membrane fragments. In agreement with a study on nonequilibrium heating in LHC II antenna complexes by transient absorption spectroscopy at various excitation intensities (*18*), this finding indicates that no global or temporary temperature increase of the sample is encountered on the time scale of the time-resolved QENS experiment under the given excitation conditions.

The reversibility of the light-induced effect can be tested by adding the QENS spectra of all neutron probe pulses obtained after laser excitation (for temporal positions, see the black diamonds in Figure 1). This data set (see frame II of Figure 2) was fit by $S_C(\mathbf{Q},\omega)$ which adopted, within experimental uncertainty, the same parameters that were used for the QENS spectrum obtained in the dark, i.e., $S_C = S_A(\mathbf{Q},\omega)$. Therefore, the changes induced by laser excitation appear to be completely reversible and yield no indication of sample denaturation under the applied excitation conditions. Note in this regard that all data sets were obtained with the same samples measured with and without time selectivity so that the experimental conditions and the applied data correction procedures are exactly the same.

In summary, our data show for the first time a light-induced transient modulation of dynamics in PS II membrane fragments. In samples with inhibited $Q_A^{-\bullet} \rightarrow Q_B$ electron transfer, this modulation appears as a reduction of the flexibility. Interestingly, this is the opposite effect compared to the transient protein softening occurring along with the large-scale structural change within the M intermediate of BR (*4*). In a complex system like PS II membrane fragments, an interpretation of this effect is not straightforward and requires further investigations, including time-resolved and laser intensity-dependent experiments. Nevertheless, it is attractive to speculate about two possible reasons for the observation of a light-induced stiffening. First, the reduced flexibility observed in this study may simply reflect a change in the protein potential landscape upon illumination, which relaxes more slowly than the excited electronic state itself. On the other hand, the flash-induced fluorescence quantum yield transients of Figure 1 indicate the formation of carotenoid triplet states (^{3}Car). Although their lifetime is much shorter than the test delay of $\sim$160 μs, conformational relaxations induced by ^{3}Car formation could have a longer lifetime. In this regard, it is interesting to note that several proposed mechanisms of photoprotection in the PS II antenna comprise aggregation-like conformational changes in the vicinity of carotenoids capable of dissipation of excess energy (*19*−*21*). Thus, the flash-induced reduction of mobility of PSII membrane fragments with blocked $Q_A^{-\bullet} \rightarrow Q_B$ electron transfer may indicate the formation of a precursor state of the predicted quenching state. However, further (laser intensity-dependent) studies are required to verify this so far speculative interpretation. Nevertheless, the observation of a reduced mobility means that the PS II protein matrix exhibits a remarkable dynamical flexibility which is capable of accommodating different functional processes. In summary, this study illustrates the potential of the novel laser−neutron pump probe technique to directly address questions about correlations between dynamic structure and function even in complex systems like PS II.

ACKNOWLEDGMENT

We are grateful to HZB Berlin for the allocation of beam time as well as to W. Altmann, T. Wilpert, W. Przybilla, G. Steiner, and B. Urban (HZB Berlin) for their technical assistance.

REFERENCES

1. Fitter, J., Lechner, R. E., and Dencher, N. A. (1999) Interactions of hydration water and biological membranes studied by neutron scattering. *J. Phys. Chem. B 103*, 8036–8050.
2. Gabel, F., Bicout, D., Lehnert, U., Tehei, M., Weik, M., and Zaccai, G. (2002) Protein dynamics studied by neutron scattering. *Q. Rev. Biophys. 35*, 327–367.
3. Doster, W., and Settles, M. (2005) Protein−water displacement distributions. *Biochim. Biophys. Acta 1749*, 173–186.
4. Pieper, J., Buchsteiner, A., Dencher, N. A., Lechner, R. E., and Hauss, T. (2008) Transient Protein Softening during the Working Cycle of a Molecular Machine. *Phys. Rev. Lett. 100*, 228103.
5. Ke, B. (2001) Photosynthesis: Photobiochemistry and Photobiophysics , Kluwer Academic Publishers, Dordrecht, The Netherlands.
6. Renger, G., and Holzwarth, A. R. (2005) Primary electron transfer. In Photosystem II: The water/plastoquinone oxido-reductase in photosynthesis (Wydrzynski, T., and Satoh, K., Eds.) pp 139−175, Kluwer Academic Publishers, Dordrecht, The Netherlands.
7. Renger, G. (2008) Functional pattern of Photosystem II in Oxygen Evolving Organisms. In Primary Processes of Photosynthesis: Basic Priniciples and Apparatus, Vol. II Reaction Centers/Photosystems, Electron Transport Chains, Photophosphorylation and Evolution (Renger, G., Ed.) pp 237−290, Royal Society of Chemistry, Cambridge, U.K.
8. Petrouleas, V., and Crofts, A. R. (2005) The iron-quinone acceptor complex. In Photosystem II: The water/plastoquinone oxido-reductase in photosynthesis (Wydrzynski, T., and Satoh, K., Eds.) pp 177−206, Kluwer Academic Publishers, Dordrecht, The Netherlands.
9. Joliot, P., and Joliot, A. (1973) Different types of quenching involved in Photosystem II centers. *Biochim. Biophys. Acta 305*, 302–316.
10. Garbers, A., Kurreck, J., Reifarth, F., Renger, G., and Parak, F. (1998) Correlation between protein flexibility and electron transfer from $Q_A^{-\bullet}$ to Q_B in PS II membrane fragments from spinach. *Biochemistry 37*, 11399–11404.
11. Pieper, J., Hauss, T., Buchsteiner, A., Baczynski, K., Adamiak, K., Lechner, R. E., and Renger, G. (2007) Temperature- and hydration-dependent protein dynamics in photosystem II of green plants studied by quasielastic neutron scattering. *Biochemistry 46*/ (40), 11398–11409.
12. Pieper, J., Hauss, T., Buchsteiner, A., and Renger, G. (2008) The effect of hydration on protein flexibility in photosystem II of green plants studied by quasielastic neutron scattering. *Eur. Biophys. J. 37*, 657–663.
13. Reinot, T., Zazubovich, V., Hayes, J. M., and Small, G. J. (2001) New Insights on Persistent Nonphotochemical Hole Burning and Its Application to Photosynthetic Complexes. *J. Phys. Chem. B 105*, 5083–5098.
14. Vass, I., and Aro, E.-M. (2008) in Primary processes of photosynthesis: Basic principles and apparatus; Photoinhibition of photosynthetic electron transport (Renger, G., Ed.) Vol. I, pp 391−424, Royal Society of Chemistry, Cambridge, U.K.
15. Garab, G., Cseh, Z., Kovács, L., Rajagopal, S., Várkonyi, Z., Wentworth, M., Mustárdy, L., Der, A., Ruban, A. V., Papp, E., Holzenburg, A., and Horton, P. (2002) Light-Induced Trimer to Monomer Transition in the Main Light-Harvesting Antenna Complex of Plants: Thermo-Optic Mechanism. *Biochemistry 41*, 15121–15129.
16. Pieper, J., Buchsteiner, A., Dencher, N. A., Lechner, R. E., and Hauss, T. (2009) Light-induced modulation of protein dynamics during the photocycle of bacteriorhodopsin. *Photochem. Photobiol. 85*, 590–597.
17. Steffen, R., Eckert, H.-J., Kelly, A. A., Dörmann, P., and Renger, G. (2005) Investigations on the reaction pattern of photosystem II in

leaves from *Arabidopsis thaliana* by time-resolved fluorometric analysis. *Biochemistry 44*, 3123–3133.
18. Gulbinas, V., Karpicz, R., Garab, G., and Valkunas, L. (2006) Nonequilibrium heating in LHC II complexes monitored by ultrafast absorption transients. *Biochemistry 45*/ (31), 9559–9565.
19. Liu, Z., Yan, H., Wang, K., Kuang, T., Zhang, J., Gui, L., An, X., and Chang, W. (2004) Crystal structure of spinach major light harvesting complex at 2.72 Å resolution. *Nature 428*, 287–292.
20. Standfuss, J., Lamborghini, M., Kuhlbrandt, W., and van Scheltinga, A. C. T. (2005) Mechanisms of photoprotection and nonphotochemical quenching in pea lightharvesting complex at 2.5 Å resolution. *EMBO J. 24*, 919–928.
21. Ruban, A. V., Berera, R., Ilioaia, C., van Stokkum, I. H. M., Kennis, J. T. M., Pascal, A. A., van Amerongen, H., Robert, B., Horton, P., and van Grondelle, R. (2007) Identification of a mechanism of photoprotective energy dissipation in higher plants. *Nature 450*, 575–578.